

# Molecular Mechanics Study of the Interaction of Thiophene with a Molybdenum Disulfide Catalyst

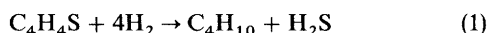
Thierry M. Brunier, Michael G. B. Drew and Philip C. H. Mitchell

Department of Chemistry, The University, Whiteknights, Reading RG6 2AD, UK

Molecular mechanics calculations have been performed to investigate the structure of the active site of a molybdenum disulfide hydrodesulfurisation catalyst and the binding of thiophene. Active sites are created by removing bridging sulfur atoms, thus exposing pairs of molybdenum atoms. Relaxing the MoS<sub>2</sub> hexagonal slabs using molecular mechanics shows that the environment of molybdenum and sulfur atoms at the active site is different from that in the bulk.

Structures of the thiophene–molybdenum disulfide active site complex have been investigated. Stable structures can be produced with the sulfur atom of thiophene attached to one or both of the coordinatively unsaturated (cus) molybdenum atoms. Our calculations show the stable configuration of thiophene at these sites. Thiophene binds through sulfur to one cus molybdenum atom with the ring either parallel to the surface (more stable) or perpendicular (slightly less stable). When the ring is perpendicular the thiophene sulfur atom can bind to the second adjacent cus molybdenum thus forming a Mo–S(thiophene)–Mo bridge. When the thiophene is parallel to the surface, bound to one molybdenum atom through sulfur, then carbon atoms of the thiophene can bind to the adjacent cus molybdenum atom. The most likely scenario for the formation of the active-site complex is for the thiophene molecule to bind perpendicular to the surface, first to one molybdenum atom and then to a second, to form an Mo–S–Mo bridge.

This paper is one of a series on the computer modelling of molybdenum disulfide catalysts. Previously we have used computer graphics and molecular mechanics to visualise and characterise active sites of molybdenum disulfide catalysts<sup>1</sup> and have parametrised molybdenum and sulfur so as to reproduce the crystal structures of MoS<sub>2</sub>.<sup>2</sup> In the present paper we report a molecular mechanics study of the structure of the active site of molybdenum disulfide and of possible active-site–thiophene complexes. Catalysts consisting of molybdenum disulfide supported on  $\gamma$ -alumina and promoted by cobalt are used for hydrodesulfurisation (HDS), the removal of sulfur compounds from crude petroleum by reaction with hydrogen.<sup>3</sup> Typical of these sulfur compounds is thiophene which undergoes HDS, ultimately to butane and hydrogen sulfide.



Thiophene has been used as a model compound in many experimental studies of the mechanism of hydrodesulfurisation.

The active phase of alumina-supported MoS<sub>2</sub> catalysts consists of hexagonal slabs of MoS<sub>2</sub> (Fig. 1) dispersed over the surface of alumina.<sup>4</sup> The active sites are cus molybdenum atoms in the slab edges. They are created by the removal of sulfur atoms when the sulfided catalyst is reduced in hydrogen. Molybdenum atoms are exposed in the (10 $\bar{1}$ 0) slab edge when singly bound sulfur is removed and in the ( $\bar{1}$ 010) edge when bridging sulfur is removed. Experimental data<sup>5</sup> show that the catalytic sites are the cus Mo atoms along the (1010) edge since HDS is optimal not at the temperature at which singly bound sulfur is removed but rather at the higher temperature when bridging sulfur is removed. The active site is therefore an ensemble comprising two molybdenum atoms within a cavity (Fig. 2).

We wish to model the mechanism of HDS using computational methods. A feature of this approach is the combination of computer graphics, which enables us to visualise structures, and established computational procedures. Accurate visualisation is especially helpful in catalytic studies where structural data may be limited or difficult to obtain. Application of computational techniques to the interaction of small molecules and surfaces has generated considerable informa-

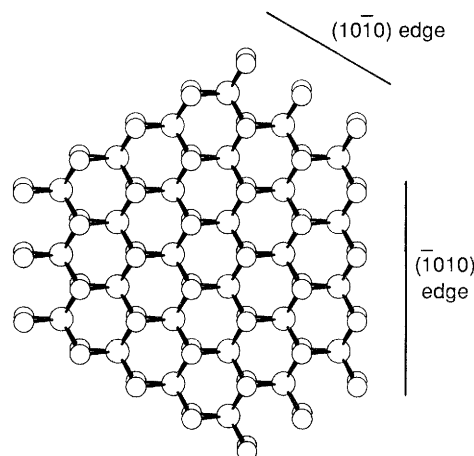


Fig. 1 Structure of a hexagonal slab cut from an MoS<sub>2</sub> layer: large circles molybdenum, small circles sulfur. This is a sulfur-rich structure; all Mo atoms, including the edge atoms, are fully coordinated and the stoichiometry is Mo<sub>27</sub>S<sub>72</sub> (i.e. MoS<sub>2.67</sub>).

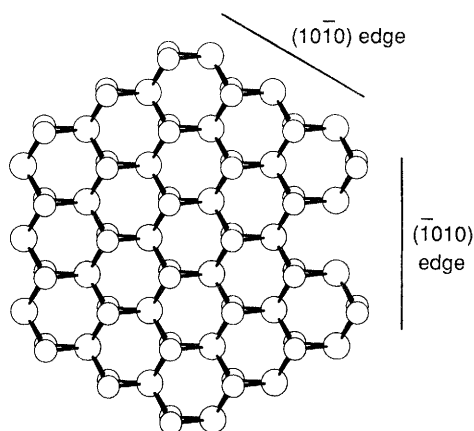


Fig. 2 Active phase of a molybdenum disulfide catalyst. All singly bound sulfur atoms were removed from the (10 $\bar{1}$ 0) edge of the saturated slab of Fig. 1 (giving a slab of stoichiometry Mo<sub>27</sub>S<sub>44</sub>, i.e. MoS<sub>2</sub>). Then a pair of bridging sulfur atoms was removed from the ( $\bar{1}$ 010) edge to create an active-site cavity.

tion on adsorption and dissociation processes.<sup>6</sup> Adsorption of unsaturated molecules like carbon monoxide, ethene and benzene at transition-metal centres is due primarily to the interaction of metal d-orbitals with the antibonding  $\pi^*$  orbitals of the adsorbate. These molecular orbitals are sufficiently low in energy to become partly occupied thus weakening the multiple bond. A similar interaction may well operate in HDS whereby thiophene is strongly adsorbed *via* metal-orbital donation of electron density into the thiophene  $\pi^*$  orbital especially in the vicinity of the C—S bonds.

Previous computational studies of the interaction of thiophene with MoS<sub>2</sub> have employed quantum mechanical calculations at various levels of sophistication.<sup>7</sup> The results of the calculations depend very much on the initial model and the procedure (Hückel, CNDO, *etc.*) used. The calculations do indicate that  $\eta^1$ -adsorbed thiophene (through S, thiophene standing perpendicular to the MoS<sub>2</sub> edge) and  $\eta^5$ -adsorbed thiophene (through the ring lying flat along the edge) are possible structures, with vertical adsorption slightly preferred. Possibly, initial adsorption occurs through  $\eta^1$  vertical adsorption and, for subsequent reaction, the adsorbed thiophene switches to  $\eta^5$  horizontal adsorption.

The broad picture which emerges from the extensive experimental data on the hydrogenation of S, O, and N compounds is that the reaction rate is affected both by the aromatic character of the molecule (less aromatic, faster hydrogenation) and by the electronegativity of the heteroatom. Possibly, hydrogenation proceeds through a  $\pi$ -adsorbed state and hydrogenolysis through a  $\sigma$ -adsorbed state. However, in the present study we investigated all the different ways in which thiophene can bind to a transition metal.

The structure of thiophene, determined by microwave spectroscopy<sup>8</sup> is shown in Fig. 3. The molecule is planar. Thiophene is a versatile ligand. In transition-metal complexes of thiophene, six different thiophene structures are known (see Fig. 4);<sup>9</sup> the thiophene molecule is seen to bind to one or more metal centres through the sulfur atom and the C=C  $\pi$  orbitals. The MoS<sub>2</sub> catalyst provides a number of thiophene-binding sites, and, by analogy with the metal complexes, the thiophene-active-site complex could involve more than one molybdenum centre bound to the thiophene. We have therefore investigated structures where thiophene can be strongly adsorbed and can interact with more than one molybdenum atom.

To model the active site, we first remove bridging sulfur atoms (Fig. 2), then we use the molecular mechanics procedure to allow the structure to relax and to establish the geometry of the active site. Using molecular graphics we dock thiophene in different ways into the active-site cavity and bind the thiophene molecule to an exposed cus molybdenum atom. This procedure provides initial sets of coordinates as input to subsequent molecular mechanics calculations. The object of the calculations is to determine an optimum structure (or structures) by an energy minimisation

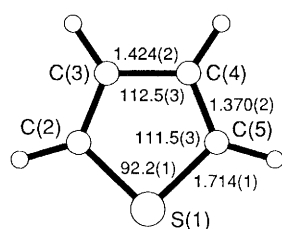


Fig. 3 The structure of thiophene determined by microwave spectroscopy (bond lengths in Å, angles in degrees)<sup>9</sup>

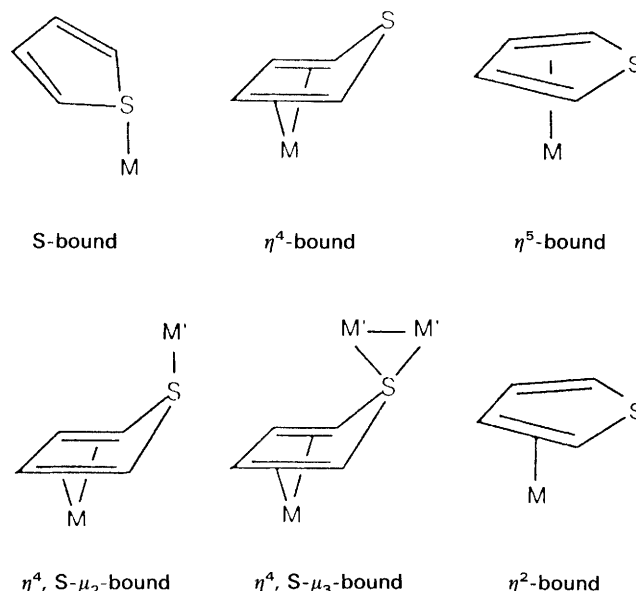


Fig. 4 Binding of the thiophene molecule to transition metals in complexes<sup>9</sup>

procedure. The optimum structure is one with minimum strain energy including both bonding and non-bonding interactions. We shall be especially concerned to determine whether one or more structures is clearly preferred.

## Computational Methods

### Computer Modelling

Computer graphics visualisation was carried out on an IBM PC-AT with the PC-CHEMMOD system.<sup>10</sup> The atomic coordinates of molybdenum disulfide were retrieved from the SERC crystallographic database<sup>11</sup> and converted into a form suitable for CHEMMOD.

### Molecular Mechanics Calculations

Molecular mechanics (MM) calculates and minimises the strain energy of a structure. A structure is treated as a collection of atoms held together by elastic (harmonic) forces which constitute the force field.<sup>12</sup> The strain energy ( $E$ ) of a structure in the force field is the sum of energy contributions from bond stretching ( $E_s$ ), angle bending ( $E_b$ ), and torsional ( $E_t$ ) motions and from non-bonded terms ( $E_{nb}$ ) which include the van der Waals attraction, the core repulsions and the Coulombic energy:

$$E = E_s + E_b + E_t + E_{nb} \quad (1)$$

The non-bonded energies between atoms  $m$  and  $n$  of type  $i$  and  $j$ , respectively, are calculated from eqn. (2):

$$E_{nb} = \sum_i \sum_j \epsilon_{mn} \{ [(r_{mn})_0 / r_{ij}]^{12} - 2[(r_{mn})_0 / r_{ij}]^6 \} + q_i q_j / r_{ij} \quad (2)$$

This energy is summed over all pairs of atoms  $i, j$  in the structure;  $m$  and  $n$  represent the atom types (*e.g.* Mo, S, C, H) of the  $i$ th and  $j$ th atoms in the structure; atoms  $i$  and  $j$  have van der Waals radii  $(r_m)_0$  and  $(r_n)_0$ , respectively. In eqn. (2) the first two terms represent a Lennard-Jones (6-12) potential;  $(r_{mn})_0$  is the sum of the van der Waals radii  $(r_m)_0$ ,  $(r_n)_0$ , for the interacting pair of atoms at a distance  $r_{ij}$ , and  $\epsilon_{mn}$  is the potential-well depth. For the two atom types,  $m$  and  $n$ ,  $\epsilon_{mn}$  is the geometric mean of the  $\epsilon$  values for each atom and the van

**Table 1** MM parameters for MoS<sub>2</sub><sup>2</sup>

Mo—S stretch	$k_s = 278.8 \text{ kcal mol}^{-1} \text{ \AA}^{-2}$	$l_0 = 2.418 \text{ \AA}$
Mo—S—Mo bend	$k_b = 0.01280 \text{ kcal mol}^{-1} \text{ degrees}^{-2}$	$\theta_0 = 81.64^\circ$
S—Mo—S bend	$k_b = 0.00950 \text{ kcal mol}^{-1} \text{ degrees}^{-2}$	$\theta_0 = 81.81^\circ, 135.65^\circ$
Mo non-bonded terms	$\epsilon = 0.2020 \text{ kcal mol}^{-1}$	$r_0 = 2.694 \text{ \AA}$
S non-bonded terms	$\epsilon = 0.4490 \text{ kcal mol}^{-1}$	$r_0 = 1.847 \text{ \AA}$
Mo—S—Mo—S torsion angles	$k_t = 0.0 \text{ kcal mol}^{-1} \text{ degrees}^{-2}$	

der Waals diameter is the sum of individual radii for atoms  $m$  and  $n$ .

$$\epsilon_{mn} = \sqrt{(\epsilon_m \epsilon_n)} \quad (3)$$

$$(r_{mn})_0 = (r_m)_0 + (r_n)_0 \quad (4)$$

In an MM calculation we start with a model structure and find the optimised geometry by minimising the total steric energy,  $E$ . To parametrise the calculation for molybdenum disulfide we need to assign values for the stretching force constant and the ideal bond length for the Mo—S bond, bending force constants and ideal Mo—S—Mo and S—Mo—S angles, torsional force constants and periodicities for Mo—S—Mo—S torsions and  $\epsilon$  and  $r_0$  for Mo and S.

MM calculations were carried out using a modified version of the CHEMMIN program<sup>13</sup> as in our earlier work on molybdenum disulfide.<sup>1,2</sup> This program uses a standard block-diagonal Newton–Raphson minimisation scheme. We used our own parameters for Mo and S (see Table 1), established by a variety of methods as reported previously.<sup>2</sup> These parameters were tested on the crystal structure of MoS<sub>2</sub> and the r.m.s. fit in coordinates between the structure minimised with MM and the crystal structure was less than 0.01 Å.

The CHEMMIN code was modified to accept our own force constants, more than one angle at molybdenum and periodic angles (*i.e.*  $\theta$  and  $2\theta$ ). The latter modifications were necessary to deal with coordination numbers greater than four.<sup>14</sup>

## Results and Discussion

### Molybdenum Disulfide Slab

Experimental data have established that there is an optimum range of slab size for the activity of the MoS<sub>2</sub> catalyst in HDS and that the 27-molybdenum-atom hexagonal slab (Fig. 1) is an appropriate active-phase model. Catalytic sites consisting of exposed molybdenum atoms were created by removing both terminal (10 $\bar{1}$ 0) sulfur and bridging ( $\bar{1}$ 010) sulfur atoms. Note that with only terminal sulfur removed the stoichiometry of the slab is Mo<sub>27</sub>S<sub>54</sub> (*i.e.* MoS<sub>2</sub>). According to the results of temperature-programmed reduction experiments of MoS<sub>2</sub> catalysts in H<sub>2</sub> the catalyst becomes active for HDS at the temperature at which bridging sulfur atoms are removed.<sup>5</sup> Since terminal sulfurs are removed at lower temperatures than bridging sulfurs, the catalytic phase presumably consists of slabs with few or no terminal sulfurs and some missing bridging sulfurs. We also assume that bridging sulfurs are removed in pairs since removing one bridging sulfur increases the lability of the second sulfur. Thus we chose our model slabs with a stoichiometry of Mo<sub>27</sub>S<sub>52</sub> consisting of a 27-molybdenum-atom slab with all (10 $\bar{1}$ 0) edge terminal sulfurs removed and the central pair of ( $\bar{1}$ 010) edge bridging sulfurs removed (Fig. 2). The relaxed slab (Fig. 5) is distorted compared with the unrelaxed slab: along (10 $\bar{1}$ 0), the Mo(4)··Mo(5) and Mo(3)··Mo(6) distances decrease (6.32 to 6.16 Å) and along ( $\bar{1}$ 010) the Mo(3)··Mo(4) distance increases (9.48 to 10.14 Å) (Fig. 5). Accordingly, although the (10 $\bar{1}$ 0) edge site shows little

rearrangement, the ( $\bar{1}$ 010) edge site is modified by a large degree of distortion. Without the bridging sulfurs, the two (cus) molybdenum atoms relax under their mutual repulsion. The Mo(1)··Mo(2) distance increases from 3.16 to 4.05 Å and the cavity is enlarged. This result agrees with our previous calculation<sup>1</sup> except that the distortion of the slab using our currently improved parameters is now smaller. These new parameters reproduce the crystal structure to within experimental error and therefore accurately represent the relative importance of the various forces in the system under static conditions.

### Thiophene–Molybdenum Disulfide Interaction

The thiophene coordinates were obtained from microwave spectroscopy (Fig. 3). The structure of thiophene was fixed; therefore all relaxation was incorporated in the molybdenum disulfide slab. The purpose of the calculations was to determine the range of configurations of thiophene that could be accommodated by the molybdenum disulfide slab on each edge where molybdenum atoms were exposed.

First, we created a model in which the sulfur atom of thiophene was bound to one molybdenum atom. The S(thiophene) thereby substitutes for one of the bridging sulfurs in the MoS<sub>2</sub> slab. Two models were considered for the interaction of thiophene with the active site in the ( $\bar{1}$ 010) edge. In model 1 (Fig. 6) the thiophene molecule lies over the cavity and parallel to the slab edge; in model 2 (Fig. 7) thiophene lies within the cavity and perpendicular to the slab.

To calculate the energies of various thiophene configurations we considered three possible Mo—S bond lengths; 2.41 Å (the distance found in MoS<sub>2</sub>), 2.155 Å (the distance found in the [MoS<sub>4</sub>]<sup>2-</sup> ion<sup>15</sup>) and 2.675 Å. We define two geometrical parameters that encompass all possible orientations, the angles  $\theta$  and  $\Phi$  of Fig. 6 and 7. The angle  $\theta$  defines the orientation of the thiophene molecule with respect to the active-site cavity;  $(180 - \theta)$  is the Mo—S—p angle, where p is the midpoint of the C(3)—C(4) bond. When  $\theta$  is zero the

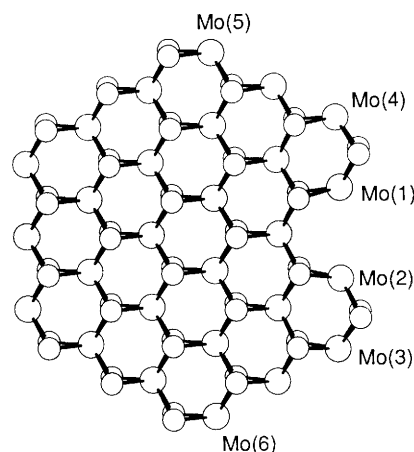


**Fig. 5** The energy-minimised structure of the MoS<sub>2</sub> active phase (*cf.* Fig. 2 for the non-minimised structure)



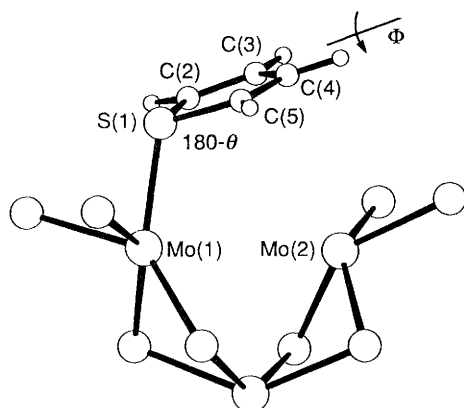


**Fig. 6** Model 1: thiophene bound through S to cus Mo at the active site and parallel to the surface.  $(180-\theta)$  is the Mo—S—p angle, where p is the midpoint of the C(3)—C(4) bond, and  $\Phi$  is the angle of rotation of the thiophene ring about the S—p vector (see text)

thiophene molecule is perpendicular to the cavity [*i.e.* to the Mo(1)··Mo(2) vector]; when  $\theta$  is  $180^\circ$  the thiophene molecule is parallel to the cavity. The angle  $\Phi$  defines the orientation of the thiophene ring relative to a plane containing the Mo(1)··Mo(2) vector and is the angle of rotation of thiophene about the S—p vector. The angle  $\Phi$  is zero when the thiophene ring and the Mo(1)··Mo(2) vector are co-planar. Structures were relaxed for the range  $0 < \theta < 110^\circ$  in steps of  $10^\circ$  and  $0 < \Phi < 90^\circ$  in steps of  $15^\circ$ . Note that for  $\Phi$  the ranges  $0-90^\circ$  and  $90-180^\circ$  are equivalent.

We thus set up  $3 \times 12 \times 7$  starting models with different values of the three geometric variables, the Mo—S bond length, and the  $\theta$  and  $\Phi$  angles. The angles  $\theta$  and  $\Phi$  were used to calculate the Mo—S—C(2) and Mo—S—C(5) angles. These two angles and the Mo—S bond length were fixed by assigning large force constants. (When bond angles are fixed, the CHEMMIN program uses by default a 1–3 non-bonded interaction term. Use of this term was not thought justifiable and it was made inoperative.)

The energy of the systems (slab-with-cavity + thiophene) was minimised keeping the thiophene structure fixed. This energy can therefore be used to calculate the interaction energy of the thiophene with the catalyst slab. To estimate this energy, we define a 'strain adsorption energy'  $E_{sa}$ :

$$E_{sa} = E(\text{slab-with-cavity} + \text{thiophene}) - E(\text{slab-with-cavity}) - E(\text{thiophene}) \quad (6)$$

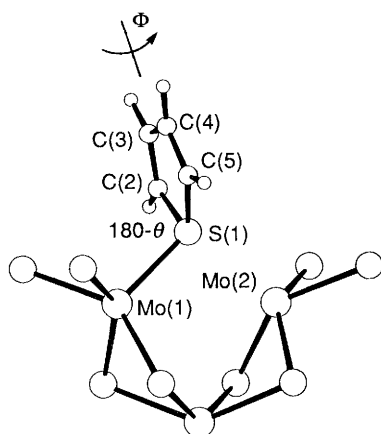


**Fig. 7** Model 2: thiophene bound through S to cus Mo at the active site and perpendicular to the surface (angles as in Fig. 6)

where the energies are strain energies calculated by MM. This equation does not include bond-formation energies since it does not take account of the energy of formation of bonds but is concerned with the steric constraints of the thiophene–active-site complexes.  $E(\text{thiophene})$  was set at  $0.0 \text{ kcal mol}^{-1}$ † as the thiophene structure was fixed in the calculations. We therefore subtracted the energy of the active site slab ( $-74.8 \text{ kcal mol}^{-1}$ ) from the energies of our models of the active-site complex to give the strain adsorption energy eqn. (6). The strain adsorption energies of the relaxed systems as a function of the angles  $\theta$  and  $\Phi$  for three Mo—S bond lengths are shown as contour maps in Fig. 8 (model 1) and Fig. 9 (model 2). The contours represent equal energies drawn at intervals of  $10.0 \text{ kcal mol}^{-1}$ .

### Thiophene Parallel to the $(\bar{1}010)$ Edge (Model 1)

The energy surface (Fig. 8) for model 1 interactions (Fig. 6) shows a well defined minimum at  $\theta = 60^\circ$ ,  $\Phi = 90^\circ$  for all three selected Mo—S(thiophene) bond distances. In the minimum-energy structure thiophene lies over the cavity slightly inclined to the  $(\bar{1}010)$  edge (Fig. 10). The energy increases as the thiophene molecule is forced towards the edge of the slab both by tilting ( $\Phi$  decreasing) and twisting ( $\theta$  increasing); at the same time the MoS<sub>2</sub> slab distorts. When  $\theta$  is large, the gradients ( $dE/d\theta$  and  $dE/d\Phi$ ) are much smaller; the thiophene molecule is then rotating above the surface.

The effect on the energy of varying the Mo—S(thiophene) bond length can be seen by comparing Fig. 8(a)–(c). The energy decreases with increasing bond length ( $-0.5 \text{ kcal mol}^{-1}$  at  $2.15 \text{ \AA}$ ,  $-3.5 \text{ kcal mol}^{-1}$  at  $2.41 \text{ \AA}$  and  $-4.0 \text{ kcal mol}^{-1}$  at  $2.67 \text{ \AA}$ ). This is because the non-bonded repulsions between thiophene and the slab are smaller at larger bond lengths. Thus a Mo—S(thiophene) bond of  $2.41 \text{ \AA}$  is acceptable for binding at this site but shorter Mo—S(thiophene) distances give rise to steeper gradients. For all three Mo—S(thiophene) distances one well defined minimum only is present. Hence the thiophene molecule does not have to climb any energy barriers to attain the minimum energy configuration. Indeed, in Fig. 11, we show the Boltzmann probability distribution at  $300 \text{ K}$  for configurations with Mo—S bonds of  $2.41 \text{ \AA}$ . This shows that all configurations at this temperature fall within a narrow range of  $\Phi$  and  $\theta$ .

### Thiophene Perpendicular to the $(\bar{1}010)$ Edge (Model 2)

For model 2 interactions (Fig. 7), the energy surfaces (Fig. 9) are similar to those for model 1 (Fig. 8). The minimum energy is at a slightly smaller value of  $\theta$  ( $45^\circ$  compared to  $60^\circ$ ) but  $\Phi$  is still  $90^\circ$ . These strain adsorption energies are much higher ( $9.6 \text{ kcal mol}^{-1}$  for Mo—S  $2.15 \text{ \AA}$ ,  $9.2 \text{ kcal mol}^{-1}$  for Mo—S  $2.41 \text{ \AA}$ ,  $11.2 \text{ kcal mol}^{-1}$  for Mo—S  $2.67 \text{ \AA}$ ) than those of model 1 ( $-0.5$ ,  $-3.5$ ,  $-4.0 \text{ kcal mol}^{-1}$ ) and the gradients at low  $\theta$  and high  $\Phi$  are smaller. In the lowest energy configuration (Fig. 12) thiophene sits vertically over the cavity such that the thiophene sulfur atom is in a position comparable to one of the bridging sulfur atoms in the  $(\bar{1}010)$  edge of the MoS<sub>2</sub> slab that has been removed to create the active site. The slab is far more distorted (Fig. 12) than in model 1, the horizontal interaction (*cf.* Fig. 10).

### Thiophene bound to the $(10\bar{1}0)$ Edge (Model 3)

Calculations were carried out for thiophene attached to molybdenum in the  $(10\bar{1}0)$  edge. The Mo—S bond length was fixed at  $2.41 \text{ \AA}$ . In Fig. 13 we show the plot of energy against

†  $1 \text{ cal} = 4.184 \text{ J}$ .

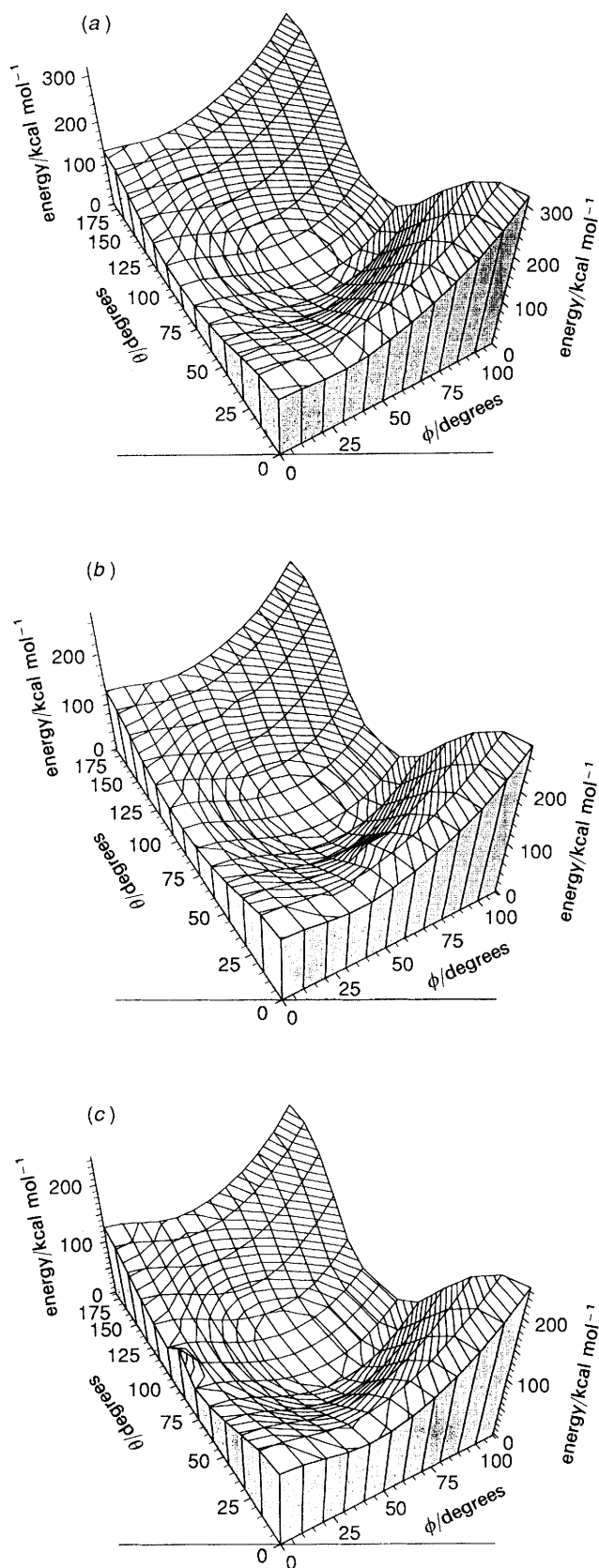


**Fig. 8** Contour plots of energy (kcal mol<sup>-1</sup>) vs. the angles  $\theta$  and  $\Phi$  for model 1 [thiophene parallel to the ( $\bar{1}010$ ) edge] for Mo-S(thiophene) distances of 2.155 Å (a), 2.41 Å (b), 2.675 Å (c)

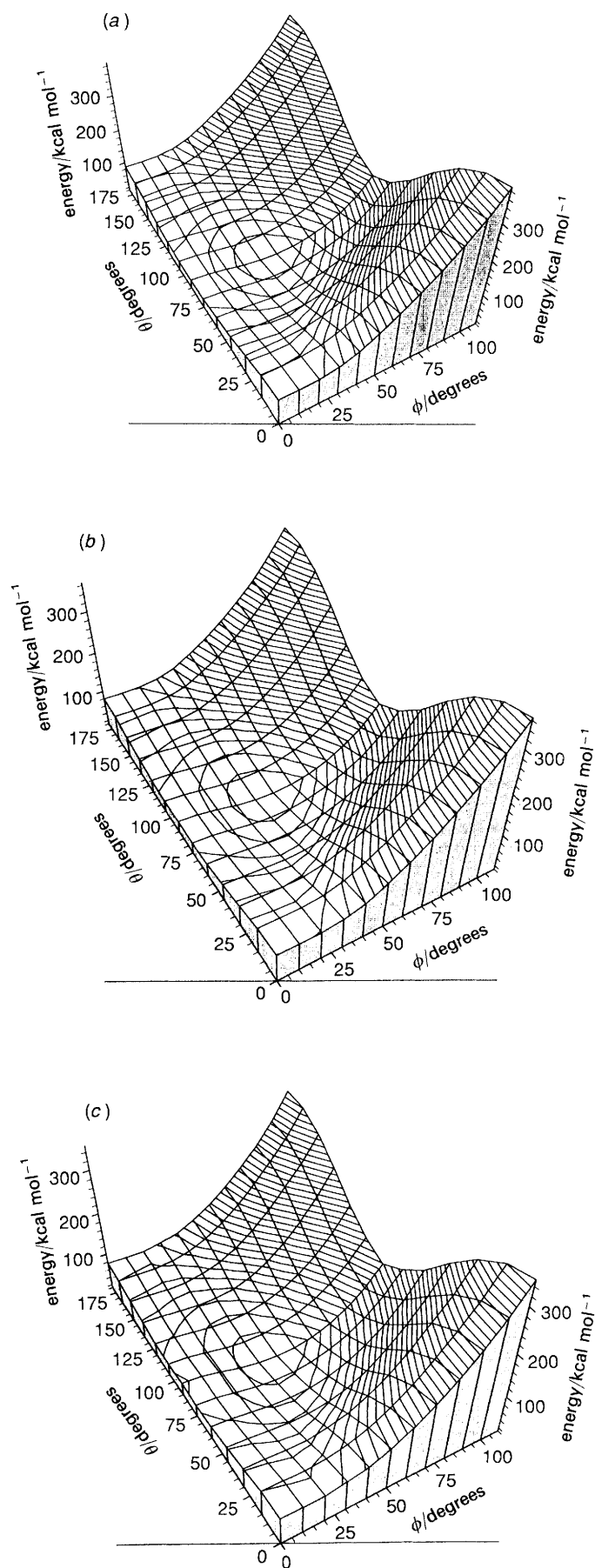


**Fig. 9** Contour plots of energy (kcal mol<sup>-1</sup>) vs. the angles  $\theta$  and  $\Phi$  for model 2 [thiophene perpendicular to the ( $\bar{1}010$ ) edge] for Mo-S(thiophene) distances of 2.155 Å (a), 2.41 Å (b), 2.675 Å (c)

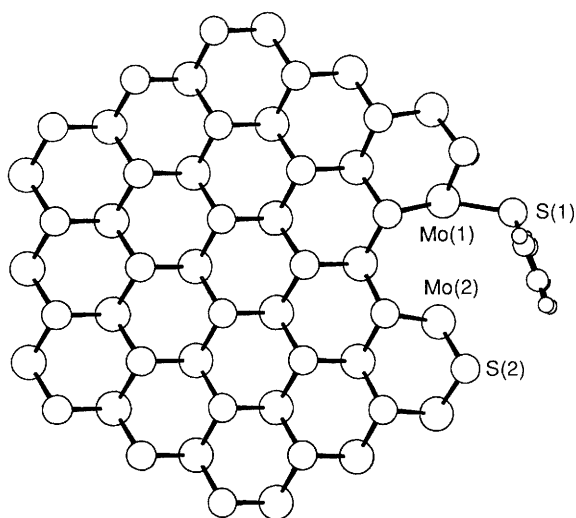


Fig. 10 Model 1: energy-minimised structure of the active-site-thiophene complex

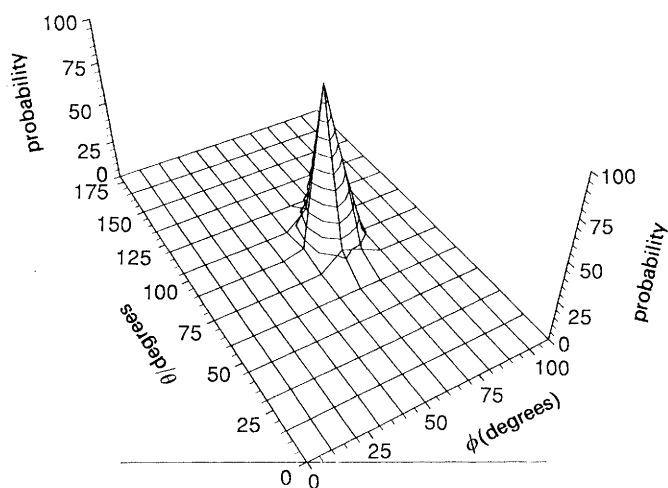


Fig. 11 Boltzmann probability distribution at 300 K of model 1 structure with Mo-S 2.41 Å

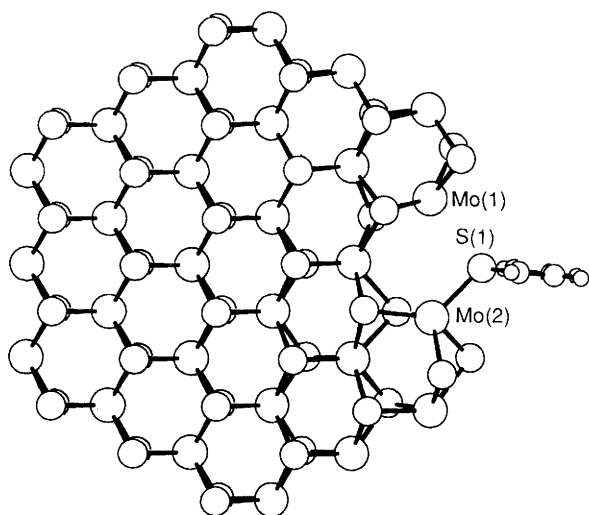


Fig. 12 Model 2: energy-minimised structure of the active-site-thiophene complex

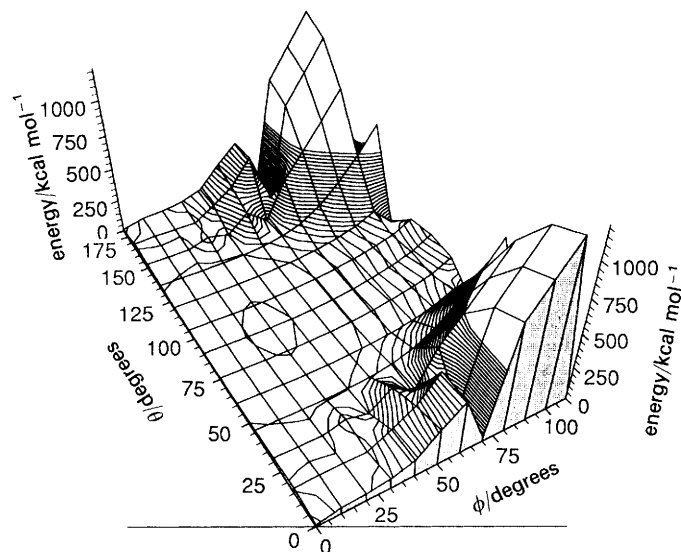


Fig. 13 Contour plot of energy ( $\text{kcal mol}^{-1}$ ) vs. the angles  $\theta$  and  $\Phi$  for model 3 [thiophene perpendicular to the (10 $\bar{1}$ 0) edge, Mo-S bond 2.41 Å]

angles  $\theta$  and  $\Phi$ . The strain adsorption energy minimum of  $-3.5 \text{ kcal mol}^{-1}$ , at angles  $\theta = 30^\circ$ ,  $\Phi = 90^\circ$  corresponds to a structure in which the thiophene molecule is standing almost perpendicular to the slab surface (Fig. 14). This energy is comparable to that found for model 1, Fig. 10, where the thiophene is parallel to the (10 $\bar{1}$ 0) edge. However, as is apparent from Fig. 14, the S(thiophene) atom in model 3 is unlikely to form a bridge to a second molybdenum atom as this would lead to a four-membered ring. We conclude that a multiple interaction is improbable on this edge which is consistent with the experimental finding that these edge sites are inactive in HDS.

#### Interaction of Bound Thiophene with a Second Molybdenum Atom in the (10 $\bar{1}$ 0) Edge

Hitherto we have regarded the interaction between the thiophene and the second cus molybdenum atom of the cavity as non-bonded. However, binding of the thiophene molecule to more than one molybdenum at the active site may be a prerequisite for the HDS process and so we now examine the

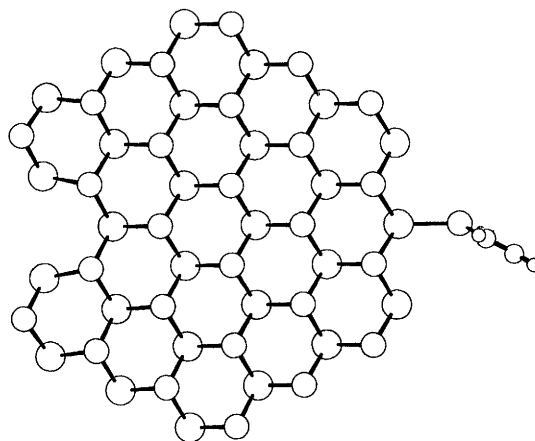


Fig. 14 Model 3: energy-minimised structure of the active-site-thiophene complex [thiophene perpendicular to the (10 $\bar{1}$ 0) edge]

consequences of the thiophene molecule in model 1 and model 2 structures binding to the second cus molybdenum atom at the active site. The MM technique cannot of course predict bond formation directly. However, by looking at possible reaction paths, it can often be concluded that the formation of a particular bond is possible or probable.

From the energy-minimised structures of model 1 and model 2 (see Fig. 10 and 12), we considered (bearing in mind the six structures of ref. 9 shown in Fig. 4) what additional bonding could result from small displacements of the thiophene molecule. In the minimised structures of models 1 and 2, the interaction between the thiophene and the second cus molybdenum atom of the cavity has been purely non-bonded and therefore the non-bonded repulsions prevented closer contact. However, if these non-bonded repulsions involve only for this model is the energy required to form the slab recovered by the adsorption of thiophene. This is an interesting result and suggests that this structure is more likely to be formed than any of the others.

We investigated models 1 and 2. From the minimum energy structure with the thiophene lying over the  $(\bar{1}010)$  edge (model 1, Fig. 10), the distances between the second cus Mo atom in the slab and the  $\alpha$ - and  $\beta$ -carbon atoms in thiophene were 3.75 and 4.12 Å, respectively. Two patterns of further bonding could be envisaged; molybdenum either bound to the two  $\beta$ -carbon atoms (model 4) or to all four carbon atoms (model 5). However, in molecular complexes of thiophene there are no precedents for either structure (see fig. 4). Although structures are known with thiophene bound to one metal atom and the four carbons to another, the two metal atoms are on opposite sides of the thiophene ring. There are no examples of structures where the  $\beta$ -carbon atoms are bound to the metal and indeed this type of bonding seems unlikely as this C—C bond has the least electron density of all the bonds in the ring.

We investigated the structures of model 4 (thiophene bound through sulfur and two  $\beta$ -carbons) and model 5 (thiophene bound through sulfur and four carbons) by MM. Mo—C bonds were included with ideal bond lengths of 2.20 Å, the sum of the Mo and C covalent radii, and were assigned the same stretching force constants as for Mo—S but the bending force constants involving these carbon atoms were set to zero.

Model 4 relaxed to an energy of  $-32.2 \text{ kcal mol}^{-1}$  giving an  $E_{\text{sa}}$  of  $42.6 \text{ kcal mol}^{-1}$ . As the refinement proceeded all four carbon atoms approached the molybdenum atom but on convergence were at a distance of 2.48 Å compared to the ideal Mo—C distance of 2.20 Å. The distance from the molybdenum atom to the  $\alpha$ -carbon atoms was 3.02 Å. The dimensions of the complex (Fig. 15) were chemically reasonable [*e.g.* Mo—C( $\beta$ )—C( $\alpha$ )  $100.0^\circ$ ; Mo—S—C( $\alpha$ )  $112.7^\circ$ ]. Model 5 refined to an energy of  $-12.9 \text{ kcal mol}^{-1}$  giving an  $E_{\text{sa}}$  of  $61.9 \text{ kcal mol}^{-1}$ . The Mo—C( $\beta$ ) distance was 2.23 Å but Mo—C( $\alpha$ ) was 2.52 Å. It is likely that closer approach of the carbons to Mo is inhibited by a close contact (2.70 Å) between an S atom of MoS<sub>2</sub> and the  $\beta$ -H atoms. These contacts are also responsible for the higher energy of model 5.

Note that the thiophene geometry is fixed in these calculations on models 4 and 5. To relieve strain the thiophene molecule could fold, with the sulfur atom coming out of the plane. Such a fold is found in the  $\eta^4\text{S}-\mu_2$  thiophene complexes but with the two metal atoms on opposite sides of the thiophene molecule. However, we found that moving the sulfur atom out of the C<sub>4</sub>S plane in models 4 and 5 increased rather than decreased the steric strain in the structure.

In these two structures the Mo···Mo distances are 3.78 Å (model 4) and 4.00 Å (model 5), values only slightly less than the value found between the cus molybdenum atoms at the

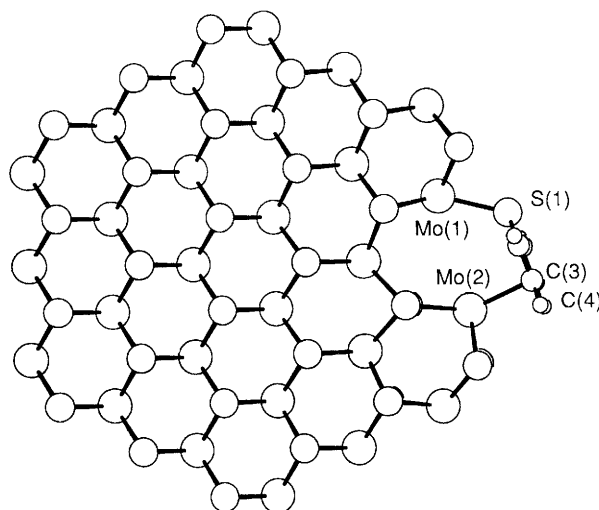


Fig. 15 Model 4: energy-minimised structure of the active-site-thiophene complex with one molybdenum atom bound to S(thiophene) and the second Mo bound to two carbons

active site but much greater than the Mo···Mo distance (3.16 Å) in the MoS<sub>2</sub> crystal structure.

By contrast with model 1, when the thiophene is positioned perpendicular to the  $(\bar{1}010)$  edge as in model 2 (Fig. 7), a likely second step is the bonding of S(thiophene) to a second molybdenum atom thereby bridging the cavity (like sulfide in the stable slab). This structure (model 6) was then minimised (Fig. 16) (energy  $-86.5 \text{ kcal mol}^{-1}$ ,  $E_{\text{sa}} -11.7 \text{ kcal mol}^{-1}$ ) and the strain in the slab due to the cavity was significantly reduced. The Mo···Mo distance was 3.25 Å, only slightly greater than the 3.16 Å found in MoS<sub>2</sub>.

### Strain Adsorption Energies

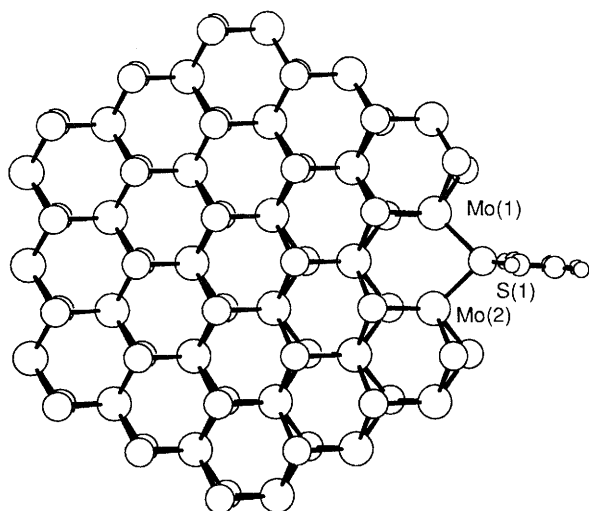
Strain adsorption energies are listed in Table 2 for our six structures (models 1–6 inclusive) described above.  $E_{\text{sa}}$  is negative (adsorption favoured) for three structures; two on the  $(\bar{1}010)$  edge, *viz.* model 1 (Fig. 10) with the thiophene singly bound through the sulfur atom ( $E_{\text{sa}} = -5.0 \text{ kcal mol}^{-1}$ ), and model 6 (Fig. 16) with S(thiophene) bridging two molybdenum atoms, ( $E_{\text{sa}} = -11.7 \text{ kcal mol}^{-1}$ ) and one structure on the  $(10\bar{1}0)$  edge, model 3 (Fig. 14), with S(thiophene) bound to one molybdenum on the  $(10\bar{1}0)$  edge ( $E_{\text{sa}} = -3.5 \text{ kcal mol}^{-1}$ ). For model 6, S(thiophene) bridging two molybdenum atoms, the energy is close to that calculated for the

Table 2 Energies of the MoS<sub>2</sub> catalyst slab and thiophene-active-site complexes

structure	figure	description	calculated energy/kcal mol <sup>-1</sup>	
			total $E_{\text{sa}}^a$	
MoS <sub>2</sub> slab				
initial	2	one cavity	-85.4	
relaxed	5	one cavity	-74.8	
thiophene-active-site complex				
model 1	10	parallel	-79.8	-5.0
model 2	12	perpendicular	-65.6	9.2
model 3	14	$10\bar{1}0$ site	-78.3	-3.5
model 4	15	S + 2C bound	-32.2	42.6
model 5		S + 4C bound	-12.9	61.9
model 6	16	S bound to 2Mo	-86.5	-11.7

<sup>a</sup> Defined by eqn. (6).  $E(\text{thiophene}) 0.0 \text{ kcal mol}^{-1}$ .





**Fig. 16** Model 6: energy-minimised structure of the active-site-thiophene complex with S(thiophene) bound to two molybdenums

original slab (Fig. 2) before the cavity was created. Therefore, only for this model is the energy required to form the slab recovered by the adsorption of thiophene. This is an interesting result and suggests that this structure is more likely to be formed than any of the others.

### Conclusions

MM has generated six structures of thiophene at the active site of a  $\text{MoS}_2$  catalyst. The least strained structure (see Table 2) has thiophene perpendicular to the active site cavity with the sulfur atom of thiophene bound to, and bridging, two molybdenum atoms (model 6, Fig. 16). Also stable, but more strained, is the structure with thiophene bound through sulfur to one molybdenum and oriented with the ring parallel with the surface (model 1, Fig. 10). Forcing the thiophene ring closer to the surface generates repulsive interactions between the thiophene molecule and surface atoms and hence strained structures. The strain may be relieved by subsequent formation of strong bonds involving the carbon atoms and  $\pi$  cloud of the thiophene ring. We are currently using quantum mechanics to investigate bonding interactions in the structures generated by our MM calculations. What is clear from

our work so far is that, in its initial interaction with an active site cavity in the (1010) edge, thiophene is likely to bind through sulfur to two proximate cus molybdenum atoms.

M.G.B.D. and P.C.H.M. thank the SERC for funds for the purchase of computer equipment and for the award of a Research Fellowship (to T.M.B.).

### References

- 1 M. G. B. Drew, P. C. H. Mitchell and S. Kasztelan, *J. Chem. Soc., Faraday Trans.*, 1990, **86**, 697.
- 2 T. M. Brunier, M. G. B. Drew and P. C. H. Mitchell, *Mol. Sim.*, 1992, in the press.
- 3 P. C. H. Mitchell, in *Catalysis (Specialist Periodical Report)*, ed. C. Kemball, The Chemical Society, London, 1977, vol. 1, p. 204; P. C. H. Mitchell, in *Catalysis (Specialist Periodical Report)*, ed. C. Kemball and D. A. Dowden, The Chemical Society, London, 1982, vol. 4, p. 175; R. Candia, O. Sorensen, J. Villadsen, N. Y. Topsøe, B. S. Clausen and H. Topsøe, *Bull. Soc. Chim. Belg.*, 1984, **93**, 783.
- 4 S. Kasztelan, H. Toulhoat, J. Grimblot and J. P. Bonelle, *Appl. Catal.*, 1984, **13**, 127.
- 5 A. Wambecke, L. Jalowiecki, S. Kasztelan, J. Grimblot and J. P. Bonnelle, *J. Catal.*, 1988, **109**, 320.
- 6 R. A. van Santen, *Theoretical Heterogeneous Catalysis*, World Scientific, Singapore, 1991, ch. 3.
- 7 C. Moreau and P. Geneste, in *Theoretical Aspects of Heterogeneous Catalysis*, ed. J. B. Moffatt, Van Nostrand Reinhold, New York, 1990, p. 256; S. Harris and R. Chianelli, p. 206.
- 8 B. Bak, D. Christensen, L. Hansen-Nygard and J. R. Rastrup-Andersen, *J. Mol. Spectrosc.*, 1961, **7**, 58.
- 9 R. J. Angelici, *Coord. Chem. Rev.*, 1990, **105**, 61.
- 10 PC-CHEMMOD System, U-micro Computers, Warrington, UK, 1987. Currently distributed by Fraser-Williams Computer Services, Poynton, Cheshire, UK.
- 11 SERC Chemical Databank System (CDS), ICSD Component, 1991 Update, SERC Daresbury Laboratory, Warrington, UK.
- 12 U. Burkert and N. L. Allinger, *Molecular Mechanics*, ACS Monograph 177, American Chemical Society, New York, 1982.
- 13 D. N. J. White, CHEMMIN Program, University of Glasgow, personal communication, 1987; D. N. J. White, J. N. Ruddock and P. R. Edgington, in *Computer Aided Molecular Design*, ed. W. G. Richards, IBC Technical Services, 1989, pp. 22–42.
- 14 M. G. B. Drew and P. C. Yates, *J. Chem. Soc., Dalton Trans.*, 1987, 2563.
- 15 H. Schafer, G. Shafer and A. Weiss, *Z. Naturforsch., Teil B*, 1964, **19**, 76; W. P. Binnie, M. J. Redman and W. J. Mallo, *Inorg. Chem.*, 1970, **9**, 1449.

Paper 2/02364D; Received 8th May, 1992